Terahertz spectroscopy and the magnetoelectric properties of manganite-based multiferroics

A A Mukhin, V Yu Ivanov, V D Travkin, A S Prokhorov, A A Volkov, A V Pimenov, A M Shuvaev, A Loidl

In this report, we present the results of magnetic, magnetoelectric, and terahertz (3–40 cm^{-1}) spectroscopic studies of several manganese multiferroics ($TbMnO_3$, $Eu_{1-x}Y_xMnO_3$, $0 < x \leqslant 0.5$) possessing a spatially modulated spin structure

(sinusoidal, cycloidal) in which, together with the usual magnetically active spin excitations, new modes, namely, electromagnons excited by an electric field, have been discovered. The behavior of these excitations in diverse spontaneous and magnetic-field-induced phase transitions and their connection with the magnetic structure have been studied. It has been established that if the modulated structure is suppressed by a magnetic field, the electromagnons disappear, and this is accompanied by significant changes in the dielectric constant of the multiferroic.

Recently, ever increasing interest has been observed in substances in which magnetic and ferroelectric orderings (multiferroics) coexist and in which the corresponding magnetic and electric degrees of freedom are coupled [1–5]. This not only governs new physical properties of such substances, but also gives the possibility of controlling their state by external magnetic or electric fields, which opens up good prospects for creating new functional materials and devices based on them.

A great response in recent years was generated by the discovery of new classes of multiferroics, in which the ferroelectric ordering has an improper nature and is connected with the specific features of the magnetic structure of these substances, while the magnetoelectric coupling is manifested substantially more strongly than in known ferroelectromagnets [6]. A common feature of such multiferroics is the presence in them of competition (frustration) of exchange interactions and the formation of incommensurate magnetic structures, including those of a cycloidal type, which possess ferroelectric properties.

Such properties were first discovered in some orthorhombic (space group of symmetry *Pbnm*) $R\mathrm{MnO_3}$ (R = Tb, Dy, Gd) manganites [7–10]. In these manganites, at temperatures below the Néel point T_N there is formed a spatially modulated sinusoidal magnetic structure with spins directed along the *b*-axis, which with a further decrease in temperature transforms either to the usual canted antiferromagnetic structure A_yF_z (Eu, Gd) or to a cycloidal (spiral) structure (Tb, Dy) [11], which possesses a spontaneous electric polarization. The reorientation of the electric polarization in a magnetic field, revealed in $\mathrm{TbMnO_3}$ and $\mathrm{DyMnO_3}$ compounds [7–9], testifies to the presence of strong magnetoelectric coupling in these multiferroics.

The presence of this strong magnetoelectric coupling must be manifested in both the static and the dynamic (spectroscopic) properties of these multiferroics and can lead to the appearance of new magnetoelectric excitations. Such spin modes excited by an electric high-frequency field, which are called electromagnons, have been revealed in $\mathrm{TbMnO_3}$ and $\mathrm{GdMnO_3}$ in a terahertz wavelength range in our recent work [12]. A characteristic property of these excitations is that they make a significant contribution to the dielectric constant of the system. Similar electroactive spin excitations were discovered later in the multiferroics $\mathrm{YMn_2O_5}$ and $\mathrm{TbMn_2O_5}$ [13], and $\mathrm{Eu_{1-x}Y_xMnO_3}$ [14–16]. Now, extensive experimental studies are being conducted in this area [17–22]. To explain the observed ferroelectric properties and magnetoelectric spin excitations in multiferroics with modulated spin structures, both phenomenological approaches [23, 24] and microscopic models [25–28] have been proposed; however, no complete explanation of these phenomena exists as yet.

In this report, we present the results of magnetic, magnetoelectric, and terahertz spectroscopic studies of several manganese multiferroics ($\mathrm{TbMnO_3}$, $\mathrm{Eu_{1-x}Y_xMnO_3}$, $0 < x \leqslant 0.5$), part of which have been published in our previous works [12, 15, 16, 20, 29–31]. The transmission spectra $T(\nu)$ were measured using the technique of quasi-optical polarization BWO spectroscopy [32, 33] (BWO is a backward-wave oscillator) in the range of frequencies $\nu = 3-40$ cm^{-1} at temperatures of 3–300 K and magnetic fields of up to 8 T. As specimens, plane-parallel oriented plates of single crystals of manganites with a thickness of about 1 mm and lateral dimensions of approximately 7–9 mm were utilized, which were grown by zone melting with radiation heating. The procedure used makes it possible to obtain spectra of the dielectric (magnetic) constant and the complete set of the parameters of resonance modes, including not only frequencies and widths of lines, but also their intensities (contributions to the dielectric or magnetic susceptibilities) [34].

Let us examine, first, the spectroscopic properties of the most studied manganite $\mathrm{TbMnO_3}$, in which at the Néel point $T_\mathrm{N} \sim 42$ K there appears initially a longitudinal sinusoidal spin-density wave with a wave vector $\mathbf{k}$ and the direction of spins of Mn^{3+} along the *crystallographic b-axis*, which, as the temperature decreases to $T \approx 27-28$ K, passes into a cycloidal structure with a vector $\mathbf{k}$ also directed along the *b*-axis; this transition is accompanied by the appearance of polarization, and for $T < 9$ K an antiferromagnetic ordering of the Tb subsystem occurs [7, 11].

Figure 1 depicts examples of the $\mathrm{TbMnO_3}$ transmission spectra taken using different geometries of experiment. A characteristic property of these transmission spectra is the presence of transmission oscillations due to the interference of the electromagnetic wave in the sample, against the background of which the resonance modes are observed. The most intense absorption lines are observed upon the $\mathbf{e} \| a$ polarization (Fig. 1c); they are virtually independent of the polarization of the high-frequency magnetic field $\mathbf{h}$ and represent electroactive modes (electromagnons) [12]. Notice the presence of a fine structure (splitting) of the electromagnon mode marked by arrows in Fig. 1. In two other polarizations, namely, $\mathbf{h} \| c$, $\mathbf{e} \| b$ and $\mathbf{h} \| b$, $\mathbf{e} \| c$, presented in Figs 1a and 1b, respectively, absorption lines are also observed at approximately the same frequencies as for the electromagnons, but their intensity is several orders of magnitude less than the intensity of the electromagnon lines. These weaker lines are identified as the modes characteristic of antiferromagnetic resonance (AFMR).

Figure 2 depicts the temperature dependences of resonance frequencies of modes observed in $\mathrm{TbMnO_3}$. Notice the coincidence of the frequencies of two AFMR modes at the polarizations $\mathbf{h} \| c$ and $\mathbf{h} \| b$ (designated by empty circles and squares) with the frequencies of the electromagnons excited in the polarization $\mathbf{e} \| a$ (shown by solid symbols), which makes it possible to suggest a mixed, magnetoactive and electroactive, nature of these excitations. An analysis reveals that the spin oscillations in this mode correspond to a deflection of the plane of the spin rotation (antiferromagnetic vector) in the cycloid from the crystal plane *bc*, which is accompanied by the appearance of a dynamic component of the electric polarization directed along the *a*-axis. Another AFMR mode (designated in Fig. 2 by triangles), which is excited only by a magnetic field $\mathbf{h} \| a$, corresponds to the oscillations of the antiferromagnetic moment in the plane *bc* of the cycloid and is a phason type mode. The lowest-frequency mode at $\mathbf{h} \| a$ (inverted triangles), which appears with the ordering of Tb^{3+} ions, is apparently connected with excitations in the rare-

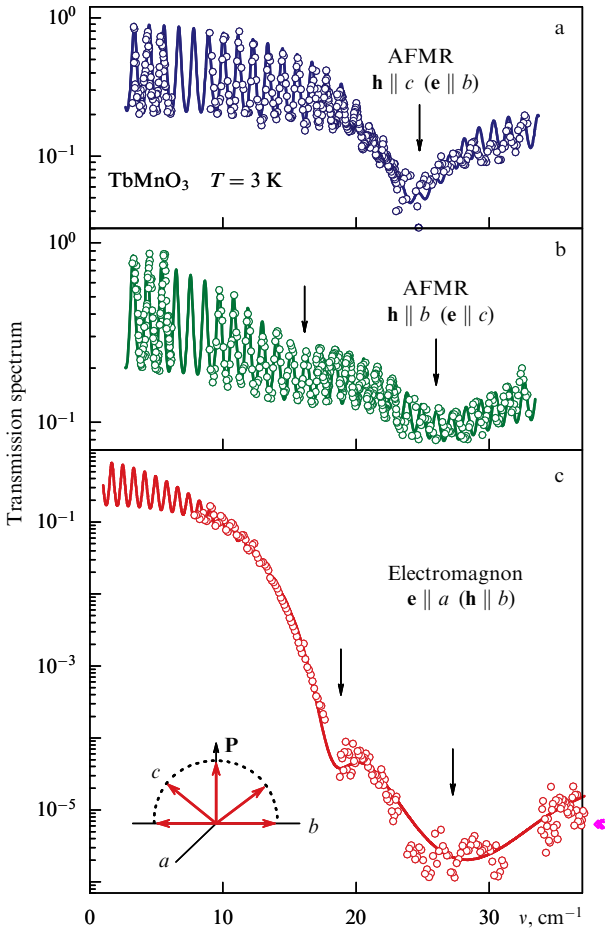

Figure 1. Transmission spectra of plane-parallel plates (~ 1 mm thick) of $TbMnO_3$ [(a, b)—*a* cut, and (c)—*c* cut] at various polarizations of electromagnetic radiation. The inset displays the cycloidal spin structure of Mn^{3+} ions and the polarization vector. Circles correspond to experimental data, while the curves to calculated results.

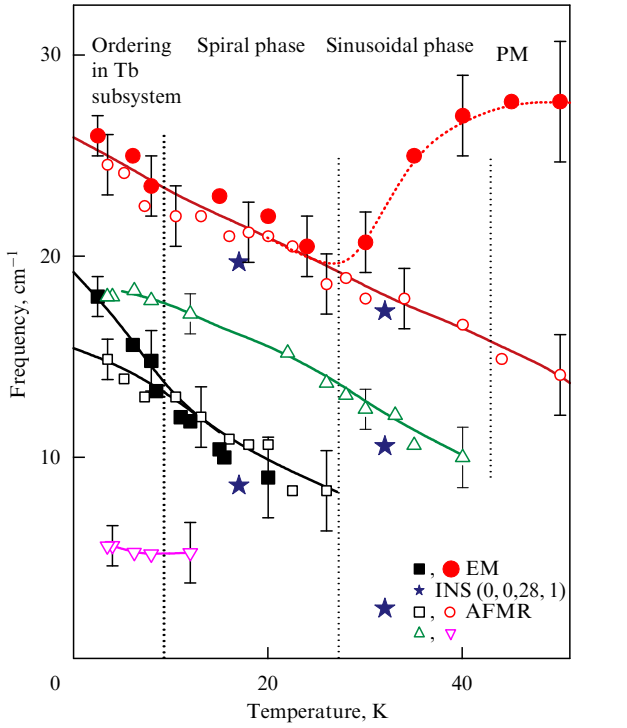

Figure 2. Temperature dependences of the resonance frequencies of various spin excitations in $TbMnO_3$. Solid circles and squares correspond to electromagnons which are observed only at $\mathbf{e} \| a$, and empty symbols correspond to magnetoactive modes of AFMR (Mn subsystem) and excitations of the Tb subsystem (circles—$\mathbf{h} \| b$ and $\mathbf{h} \| c$; squares—$\mathbf{h} \| b$, and triangles—$\mathbf{h} \| a$). In the sinusoidal phase for $T > 27$ K, the frequency positions of the electromagnons are determined only poorly because of a strong broadening; an increase in their frequency reflects in fact the strong increase in their linewidth upon transition to the paramagnetic phase. Asterisks correspond to data on inelastic neutron scattering (INS) [18, 19]. The lines are drawn through the data points only as a guide for eye. The vertical dotted lines separate different phases.

earth subsystem. In the cycloidal ferroelectric phase, the frequencies of the electromagnons and AFMR are sufficiently well identified, in spite of their noticeable widths, but upon transition to the sinusoidal phase for $T > 27$ K the frequency position of the electromagnons is now no longer very definite because of the strong broadening; therefore, the increase in their frequency (see Fig. 2) reflects in fact a strong increase in the linewidth. Note also that at the transition to the paramagnetic phase a noticeable absorption is observed, which appears to be connected with spin fluctuations; in Fig. 2 this is reflected in some curves going into the temperature range that exceeds T_N.

Also shown in Fig. 2 (asterisks) are the frequencies of some modes observed in $TbMnO_3$ with the aid of the inelastic neutron scattering (INS) method [18, 19], which on the whole agree with the excitations discovered by us. Worthy of note is the fact that these modes correspond to inhomogeneous oscillations with the wave vector $k_0 \approx 0.28$ directed along the *b*-axis, which coincides with the wave vector $\mathbf{k}_m$ of the static modulated magnetic structure, $k_m \approx k_0$. Therefore, the excitation of these oscillations in the quasioptical spectra by a practically uniform electromagnetic field with a wave vector $k_{ph} \approx 0$ is accomplished with the participation of Umklapp processes and does not violate the law of conservation of momentum: $k_{ph} = k_m - k_0 \approx 0$.

Examples of the manifestation of electromagnons in the spectra of the real and imaginary parts of the dielectric constant $\varepsilon(\nu) = \varepsilon_1(\nu) + i\varepsilon_2(\nu)$ and their suppression in a magnetic field $\mathbf{B} \| c$ are illustrated in Fig. 3. It is seen that two electromagnon modes observed at $B = 0$ at frequencies of 16 and 24 cm^{-1} disappear upon application of a magnetic field of 8 T along the *c*-axis; under its action, the cycloidal spin structure passes into a usual canted antiferromagnetic phase [8, 9, 12]. In the magnetic field directed along *a*- or *b*-axis, which induces the reorientation of the spin cycloid into the plane *ab*, and of the spontaneous polarization from *c*-axis to *a*-axis, the electromagnon modes are retained and become split into several components [31]. This is indicative of a close interconnection between the electromagnons and the spin structure of the system.

Let us now examine the magnetoelectric and terahertz spectroscopic properties of the new family of multiferroics on the base of yttrium-doped $Eu_{1-x}Y_xMnO_3$ manganites ($0 < x \leqslant 0.5$) [15, 16, 29, 30]. An attractive feature of this system is that it presents the possibility of purposefully controlling and changing the type of magnetic ordering—from the canted antiferromagnetic phase to the spatially modulated magnetic structures that possess a spontaneous electric polarization—by varying the degree of orthorhombic distortions of the crystal lattice and Mn–O–Mn bond angles determining the relationships between the different

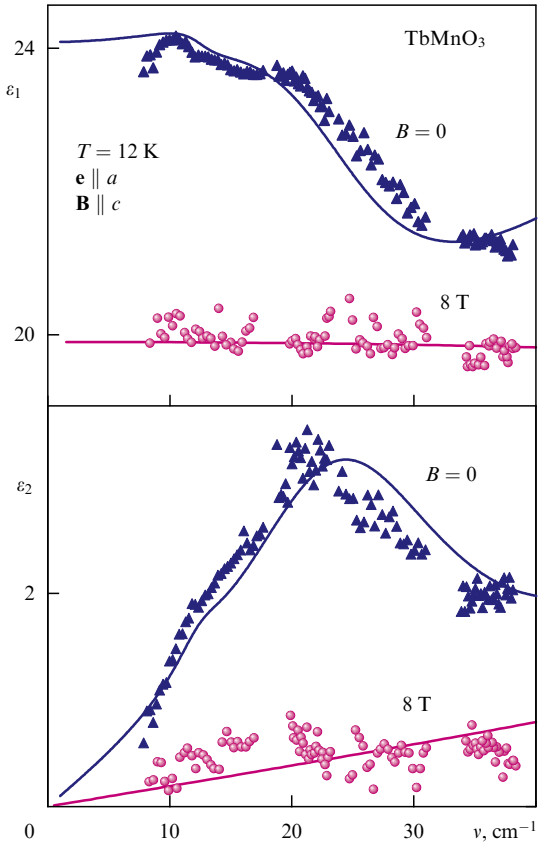

Figure 3. Suppression of electromagnons in a magnetic field $\mathbf{B} \| c$ in the spectra of the real and imaginary parts of the dielectric constant $\varepsilon(\nu) = \varepsilon_1(\nu) + i\varepsilon_2(\nu)$ along the a-axis. In a field of 8 T, the cycloidal spin structure passes into the usual canted antiferromagnetic phase in which the electromagnon disappears.

contributions to the exchange interactions. Furthermore, rare-earth magnetism is virtually absent in this system, which makes it possible to directly follow the Mn subsystem. Studies of magnetic, dielectric, and ferroelectric properties of these systems have revealed the existence of diverse spontaneous and field-induced phase transitions, which indicate the occurrence of a close interconnection between the electric polarization and the magnetic structure [29, 30].

Figure 4a illustrates the examples of temperature dependences of magnetization σ in the magnetic field of 10 kOe, dielectric constants ε, and polarizations P of the crystal $Eu_{0.6}Y_{0.4}MnO_3$. It is seen that the transition to the sinusoidal incommensurate (IC) phase causes a bend in the $\sigma_b(T)$ dependence at T_N, and the subsequent transition to the ferroelectric (FE) cycloidal phase at T_{FE} is accompanied not only by the appearance of polarization P, but also by anomalies in $\sigma_a(T)$, $\varepsilon_a(T)$, and $\varepsilon_c(T)$. Near T_{FE}, a spontaneous reorientation of polarization was revealed from the c-axis to a-axis. At small concentrations ($x < 0.2$), the ground state at low temperatures is already the usual canted antiferromagnetic (CAF) structure into which the system passes from the sinusoidal paraelectric phase. In the intermediate region ($x \sim 0.2$), the behavior of the system has a clearly pronounced hysteretic nature and depends on the sample prehistory: when cooling in the absence of a field, an FE phase is realized up to quite low temperatures, while upon cooling in a rather weak field $\mathbf{H} \| c$ (~ 1 kOe) a transition to a canted antiferromagnetic phase occurs. Figure 4b displays the

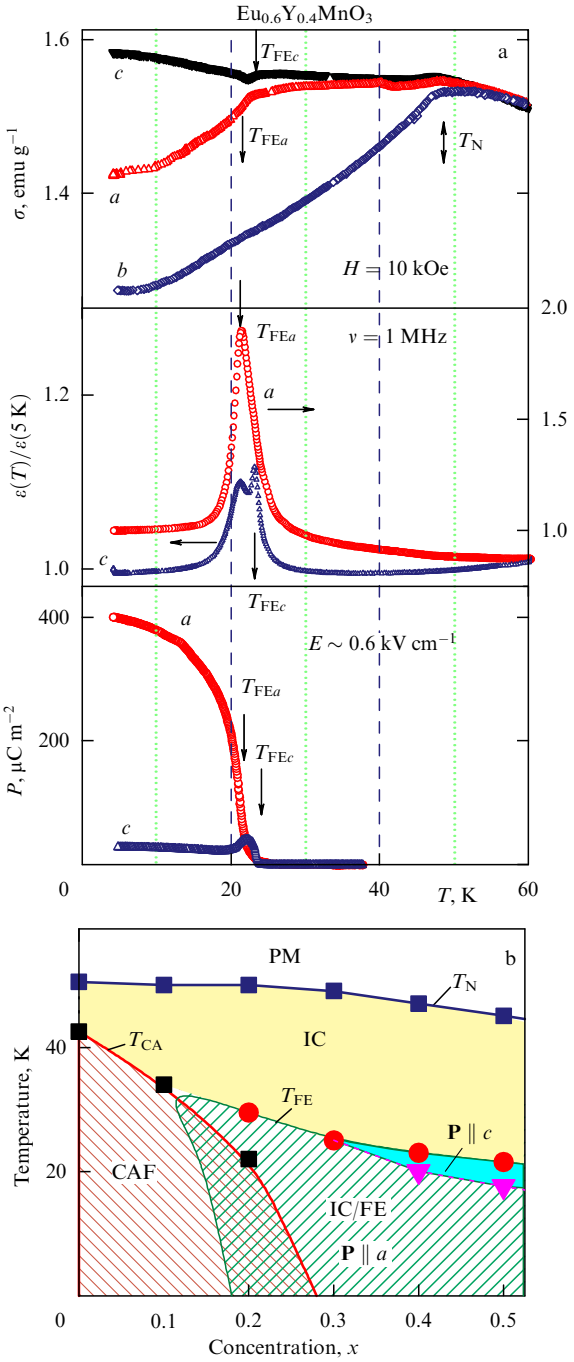

Figure 4. (a) Temperature dependences of the magnetization σ (in a field of 10 kOe), dielectric constant ε (at a frequency $\nu = 1$ MHz), and electric polarization P of an $Eu_{0.6}Y_{0.4}MnO_3$ crystal. The symbols a, b, and c alongside the curves correspond to the crystallographic axis along which the corresponding quantities were measured. In pyroelectric measurements of the polarization, the crystal was preliminarily cooled in an electric field $E \approx 0.6$ kV cm^{-1}. The vertical arrows point to phase transitions. (b) A $T-x$ phase diagram of the $Eu_{1-x}Y_xMnO_3$ system: PM stands for the paramagnetic phase; IC, sinusoidal incommensurate phase; IC/FE, spiral ferroelectric (cycloidal) phase, and CAF, canted antiferromagnetic phase.

$T-x$ phase diagram which illustrates the magnetic and electric states discovered in the $Eu_{1-x}Y_xMnO_3$ system.

Let us now turn to the terahertz spectroscopic properties of $Eu_{1-x}Y_xMnO_3$ compound (see also Refs [15, 16]). Figure 5a displays transmission spectra for a weakly doped $Eu_{0.9}Y_{0.1}MnO_3$ in the polarization $\mathbf{e} \| a$, $\mathbf{h} \| c$, in which,

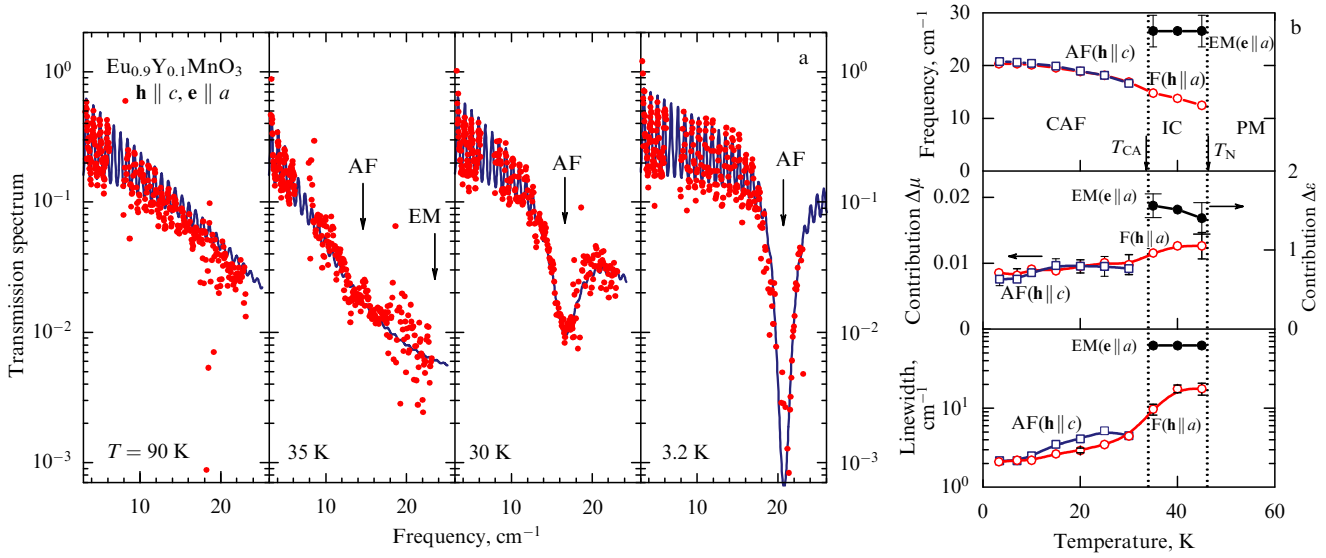

Figure 5. (a) Temperature evolution of the transmission spectra of $Eu_{0.9}Y_{0.1}MnO_3$ in the polarization $\mathbf{e} \parallel a$, $\mathbf{h} \parallel c$ in the course of phase transitions from the paramagnetic (PM) state to a sinusoidal incommensurate (IC) phase and then to a canted antiferromagnetic (CAF) state: points correspond to experimental results, and curves to theoretical calculations. (b) Temperature dependences of resonance frequencies, linewidths, and corresponding contributions to the permittivity or permeability from the electromagnon (EM) and quasiferromagnetic (F) and quasiantiferromagnetic (AF) modes of the AFMR. Vertical dotted lines denote phase boundaries.

according to the phase diagram, a phase transition first occurs to the IC phase and then to the usual CAF state. It is seen that, as the temperature decreases, a wide absorption band appears in the sinusoidal phase (at $T \approx 35$ K), which represents an electromagnon (EM) mode excited by a high-frequency field $\mathbf{e} \parallel a$. Upon phase transition to the canted antiferromagnetic phase, the electromagnon disappears, the sample becomes more transparent, and a relatively narrow absorption line appears (at $T \approx 30$ K), which represents a quasiantiferromagnetic AFMR mode excited by the magnetic field $\mathbf{h} \parallel c$. With a further decrease in temperature, the frequency of this mode grows and the width diminishes.

Figure 5b depicts the temperature dependences of the parameters of the electromagnon and quasiferromagnetic (F) and quasiantiferromagnetic (AF) modes of AFMR, which were obtained by processing transmission spectra with the use of the oscillator model for the frequency dispersion of the permittivity (ε) and permeability (μ). Note the relaxation nature of the electromagnon mode whose linewidth exceeds the frequency, and also the noticeable contribution of this mode, $\Delta\varepsilon \sim 1.5$, to the permittivity. Worthy of note is also a considerable decrease in the linewidths of the F and AF modes of the AFMR upon transition to the canted antiferromagnetic state.

At higher yttrium concentrations, when a cycloidal ferroelectric phase with a polarization along the a-axis becomes the ground state of the system at low temperatures, the electromagnons, as in $TbMnO_3$, represent well identified intense resonance modes observed at $\mathbf{e} \parallel a$. Figure 6 gives, as an example, the low-temperature spectra of the real and imaginary parts of the dielectric constant of an $Eu_{1-x}Y_xMnO_3$ compound at $x = 0.2$ and 0.5, which clearly demonstrate these modes. They have close frequencies, and their contribution to the dielectric constant grows substantially with an increase in the concentration x (from $\Delta\varepsilon \sim 2$ at $x = 0.2$ to $\Delta\varepsilon \sim 7-8$ at $x = 0.5$), which points to the enhancement of the corresponding magnetoelectric interaction.

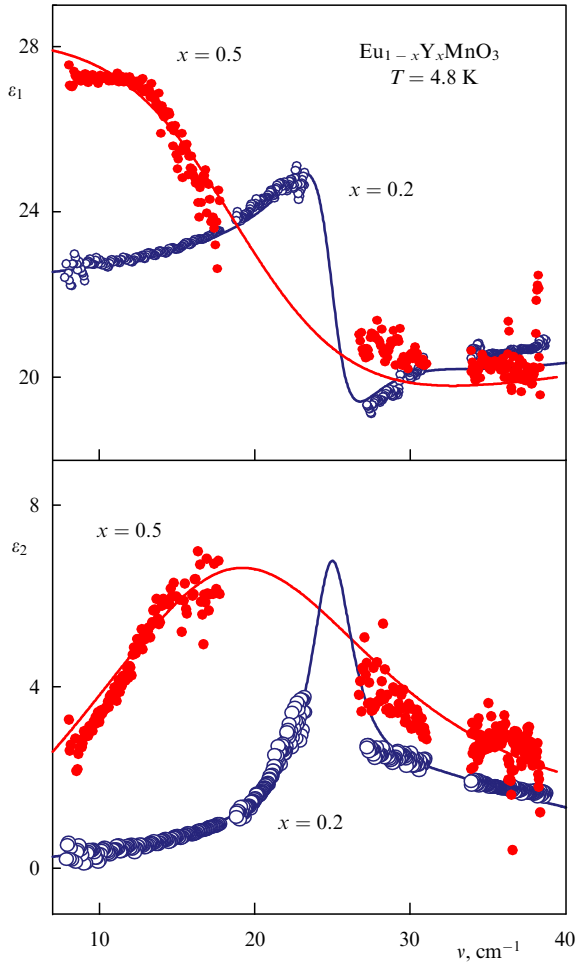

Figure 6. Electromagnon mode in the spectra of the real (ε_1) and imaginary (ε_2) parts of the dielectric constant $\varepsilon(\nu) = \varepsilon_1(\nu) + i\varepsilon_2(\nu)$ along the a-axis of the multiferroics $Eu_{1-x}Y_xMnO_3$ at $x = 0.2$ and 0.5 in the cycloidal ferroelectric phase. Points correspond to experimental data, and curves to calculated results.

Although no consistent microscopic theory for describing the mechanisms of the appearance of ferroelectricity and dynamic coupling in the multiferroics studied has yet been developed, it is already clear that the electric polarization vector appears as a result of breaking the centrosymmetricity of the system due to the appearance (in a specific temperature interval) of cycloidal magnetic structures incommensurate with the crystal lattice. At present, the most widely applied mechanism is the exchange-relativistic inhomogeneous magnetoelectric interaction which leads to the appearance of a local polarization vector $\mathbf{p} \quad \mathbf{e}_{ij}[\mathbf{S}_i\mathbf{S}_j]$ with a noncollinear arrangement of the adjacent spins, where $\mathbf{e}_{ij}$ is the vector that connects spins $\mathbf{S}_i$ and $\mathbf{S}_j$ [23, 25, 26] (Dzyaloshinskii–Moriya exchange interaction). The total polarization vector for this cycloidal structure proves to be proportional to the vector product of the wave vector $\mathbf{k}$ of the magnetic structure and the normal $\mathbf{e}$ to the plane of the spin rotation: $\mathbf{P} \sim [\mathbf{ek}]$ [23]. In the continuum approximation, as follows from a group-theoretical analysis, the observed ferroelectric properties of these multiferroics are caused by a Lifshitz type inhomogeneous magnetoelectric interaction:

$$\Phi_{\text{me}} = -a_x P_x \quad A_x \frac{\partial A_y}{\partial y} - A_y \frac{\partial A_x}{\partial y}$$

$$- a_z P_z \quad A_z \frac{\partial A_y}{\partial y} - A_y \frac{\partial A_z}{\partial y} \quad ,$$

where $\mathbf{A}$ is the antiferromagnetic vector [12, 20], which both leads to a spontaneous polarization and determines the contribution to the dielectric constant and the coupling of the homogeneous electric field with spin excitations. With this type of magnetoelectric interaction, the change in the plane of rotation of Mn^{3+} spins in the cycloid from *bc* to *ab* should lead to a change in the excitation condition of electromagnons ($\mathbf{e} \| a \rightarrow \mathbf{e} \| c$); however, as follows from our and other investigations, this is not the case, and the electromagnons are observed only at the $\mathbf{e} \| a$ polarization. This means that another type of magnetoelectric coupling can also exist, which has been suggested recently in Ref. [22]. This type of magnetoelectric coupling, which has an exchange origin, is related to specific features of the crystal structure and determines the contribution to the dielectric constant along the *a*-axis irrespective of the cycloid orientation. However, as was revealed, this contribution comes only from high-lying spin excitations corresponding to the Brillouin zone boundary. Therefore, there is no full understanding of what role is played by the magnetoelectric interactions of this type in the formation of the electromagnon response, and the problem calls for additional investigations.

Acknowledgments

This work was supported in part by the Russian Foundation for Basic Research (project Nos 09-02-01355 and Bel_a-08-02-90060) and by the Program Kvantovaya Makrofizika (Quantum Macrophysics) of the Russian Academy of Sciences.

References

1. Fiebig M *J. Phys. D* **38** R123 (2005)
2. Tokura Y *Science* **312** 1481 (2006)
3. Cheong S-W, Mostovoy M *Nature Mater.* **6** 13 (2007)
4. Khomskii D I *J. Magn. Magn. Mater.* **306** 1 (2006)
5. Ramesh R, Spaldin N A *Nature Mater.* **6** 21 (2007)
6. Smolenskii G A, Chupis I E *Usp. Fiz. Nauk* **137** 415 (1982) [*Sov. Phys. Usp.* **25** 475 (1982)]
7. Kimura T et al. *Nature* **426** 55 (2003)
8. Goto T et al. *Phys. Rev. Lett.* **92** 257201 (2004)
9. Kimura T, Lashley J C, Ramirez A P *Phys. Rev. B* **73** 220401(R) (2006)
10. Kadomtseva A M et al. *Pis'ma Zh. Eksp. Teor. Fiz.* **81** 22 (2005) [*JETP Lett.* **81** 19 (2005)]
11. Kenzelmann M et al. *Phys. Rev. Lett.* **95** 087206 (2005)
12. Pimenov A et al. *Nature Phys.* **2** 97 (2006)
13. Sushkov A B et al. *Phys. Rev. Lett.* **98** 027202 (2007)
14. Aguilar R V et al. *Phys. Rev. B* **76** 060404(R) (2007)
15. Pimenov A et al. *Phys. Rev. B* **77** 014438 (2008)
16. Mukhin A A et al. *Izv. Ross. Akad. Nauk Ser. Fiz.* **71** 1658 (2007) [*Bull. Russ. Acad. Sci. Phys.* **71** 1617 (2007)]
17. Kida N et al. *Phys. Rev. B* **78** 104414 (2008)
18. Senff D et al. *Phys. Rev. Lett.* **98** 137206 (2007)
19. Senff D et al. *J. Phys. Condens. Matter* **20** 434212 (2008)
20. Pimenov A et al. *J. Phys. Condens. Matter* **20** 434209 (2008)
21. Takahashi Y et al. *Phys. Rev. Lett.* **101** 187201 (2008)
22. Aguilar R V et al. *Phys. Rev. Lett.* **102** 047203 (2009)
23. Mostovoy M *Phys. Rev. Lett.* **96** 067601 (2006)
24. Harris A B *Phys. Rev. B* **76** 054447 (2007)
25. Katsura H, Nagaosa N, Balatsky A V *Phys. Rev. Lett.* **95** 057205 (2005)
26. Sergienko I A, Dagotto E *Phys. Rev. B* **73** 094434 (2006)
27. Katsura H, Balatsky A V, Nagaosa N *Phys. Rev. Lett.* **98** 027203 (2007)
28. Chenglong Jia et al. *Phys. Rev. B* **76** 144424 (2007)
29. Ivanov V Yu et al. *J. Magn. Magn. Mater.* **300** e130 (2006)
30. Hemberger J et al. *Phys. Rev. B* **75** 035118 (2007)
31. Pimenov A et al. *Phys. Rev. Lett.* **102** 107203 (2009)
32. Volkov A A et al. *Infrared Phys.* **25** 369 (1985)
33. Kozlov G V, Volkov A A "Coherent source submillimeter wave spectroscopy", in *Millimeter and Submillimeter Wave Spectroscopy of Solids* (Ed. G Grüner) (Berlin: Springer, 1998) p. 51
34. Gorshunov B et al. *Int. J. Infrared Millimeter Waves* **26** 1217 (2005)